Electronic Supplementary Information

Effect of side chain length on charge transport, morphology, and photovoltaic performance of conjugated polymers in bulk heterojunction solar cells

Chunhui Duan, Robin E. M. Willems, Jacobus J. van Franeker, Bardo J. Bruijnaers, Martijn M. Wienk, and René A. J. Janssen*

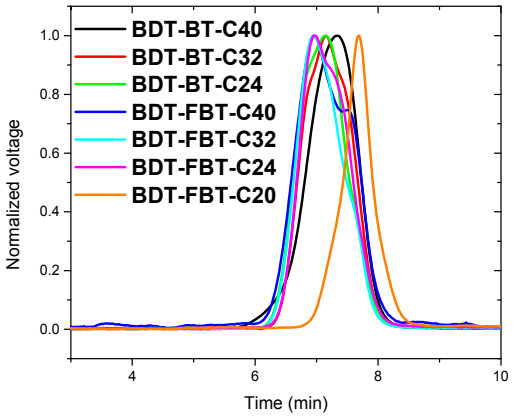

Fig. S1 GPC traces of the BDT-BT-C*n* polymers and BDT-FBT-C*n* polymers with o-DCB as eluent at 140 °C.

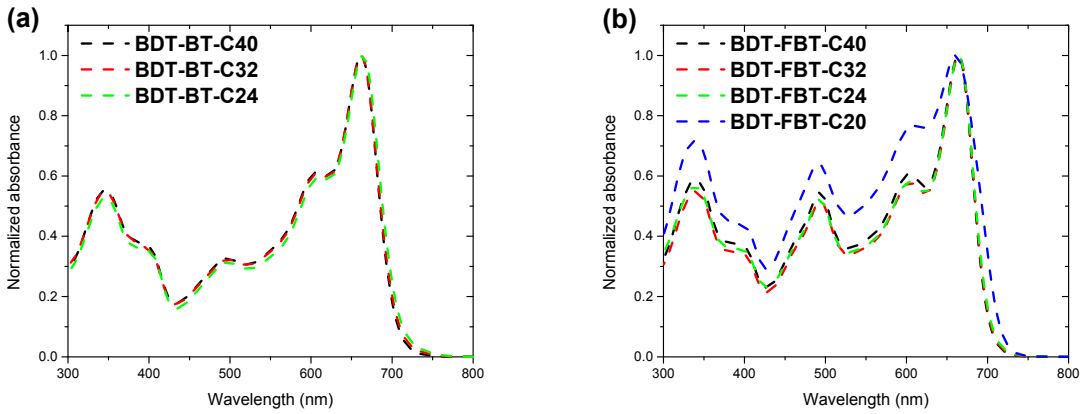

Fig. S2 UV-vis absorption spectra of (a) BDT-BT-C40, BDT-BT-C32, BDT-BT-C24, and (b) BDT-FBT-C40, BDT-FBT-C32, BDT-FBT-C24, BDT-FBT-C20 in *o*-DCB solutions with concentration of 0.05 mg mL^{-1}.

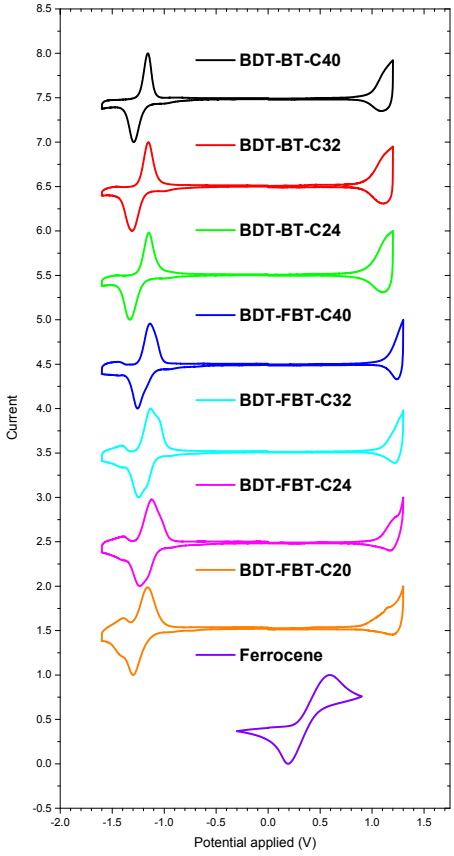

Fig. S3 Cyclic voltammograms of BDT-BT-C40, BDT-BT-C32, BDT-BT-C24, BDT-FBT-C40, BDT-FBT-C32, BDT-FBT-C24, BDT-FBT-C20, and ferrocene measured in acetonitrile.

Table S1 Performances of the solar cells based on BDT-FBT-C24 fabricated from different conditions under AM1.5G illumination (100 mW cm^{-2}). The device structure is ITO/PEDOT:PSS/active layer/ECL/Al.

ECL	Acceptor	D:A	Solvent	Annealing	J_{sc} (mA cm^{-2})	V_{oc} (V)	FF	PCE (%)
LiF	[60]PCBM	1:1.5	*o*-DCB	-	6.9	0.99	0.51	3.5
			CB	-	7.4	0.89	0.55	3.7
		1:2	CB	-	7.2	0.99	0.58	4.1
				100 °C, 10 min	7.6	0.97	0.50	3.7
			CB (2% CN)	-	7.6	0.97	0.58	4.3
		1:2.5	CB	-	6.2	0.98	0.61	3.7
	[70]PCBM	1:2	CB	-	6.0	0.96	0.54	3.1
PFN	[60]PCBM	1:2	CB	-	8.4	0.99	0.62	5.1
			CB (2.5% DIO)	-	8.3	0.95	0.57	4.5

Table S2 Performances of the solar cells processed from CB (2.5% DIO) under AM1.5G illumination (100 mW cm^{-2}). The device structure is ITO/PEDOT:PSS/active layer/ECL/Al.

Polymer	ECL	J_{sc} (mA cm^{-2})	V_{oc} (V)	FF	PCE (%)
BDT-BT-C40	PFN	4.8	0.90	0.42	1.8
BDT-BT-C32		7.2	0.89	0.57	3.7
BDT-BT-C24		10.9	0.87	0.64	6.1
BDT-FBT-C40		6.7	0.93	0.61	3.8
BDT-FBT-C32		6.9	0.94	0.56	3.6
BDT-FBT-C24		8.3	0.95	0.57	4.5
BDT-FBT-C20	LiF	5.3	0.93	0.51	2.5

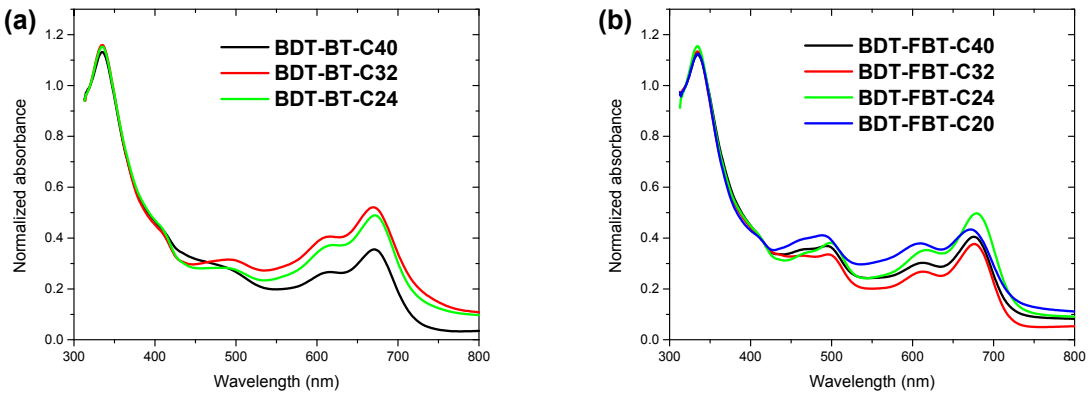

Fig. S4 UV-vis absorption spectra of the polymer:[60]PCBM blends (i.e., the active layers) on glass substrates. The spectra are normalized to [60]PCBM peak at 320 nm.

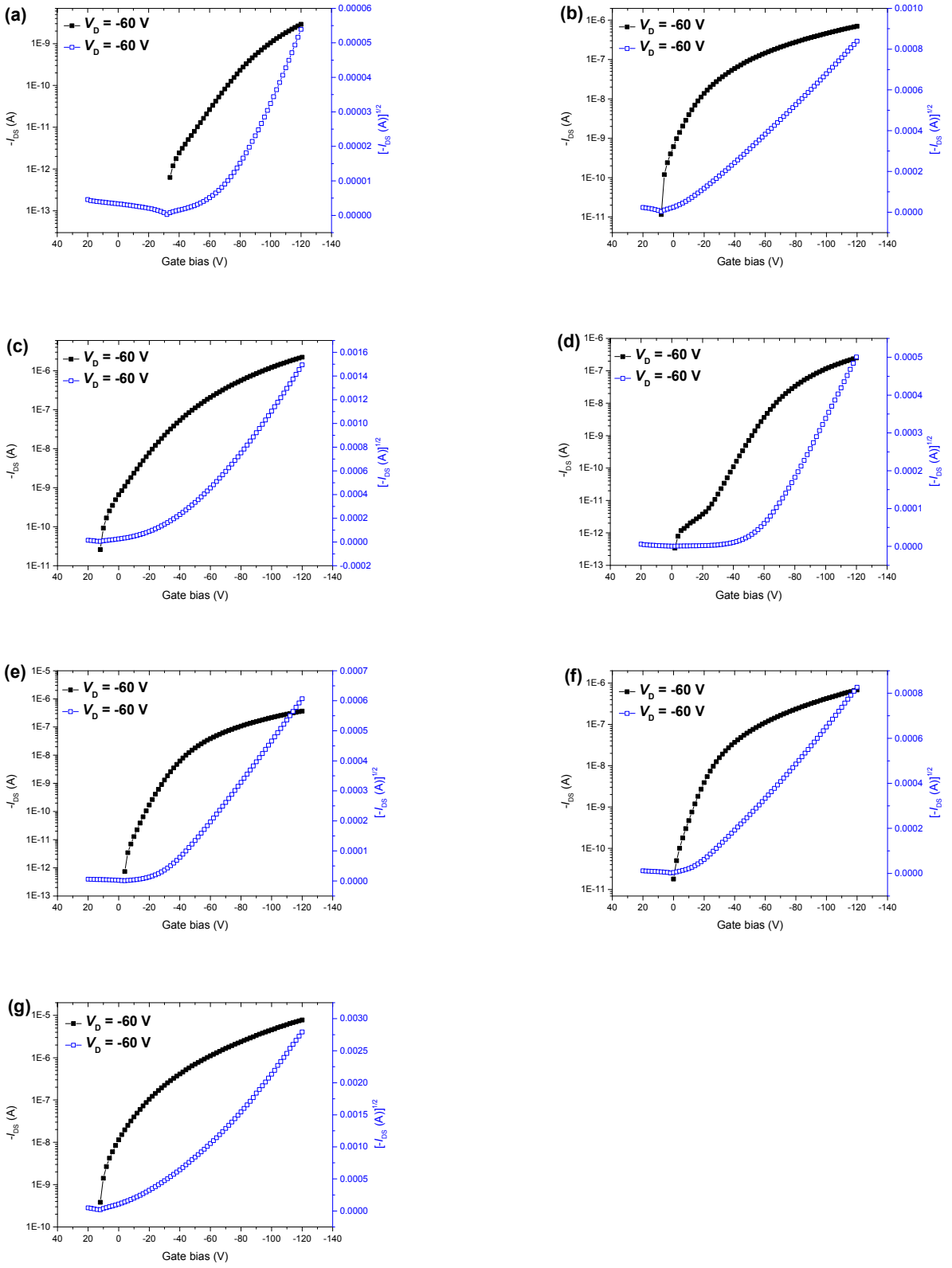

Fig. S5 Transfer characteristics of FETs made from BDT-BT-C40 (a), BDT-BT-C32 (b), BDT-BT-C24 (c), BDT-FBT-C40 (d), BDT-FBT-C32 (e), BDT-FBT-C24 (f), and BDT-FBT-C20 (g).

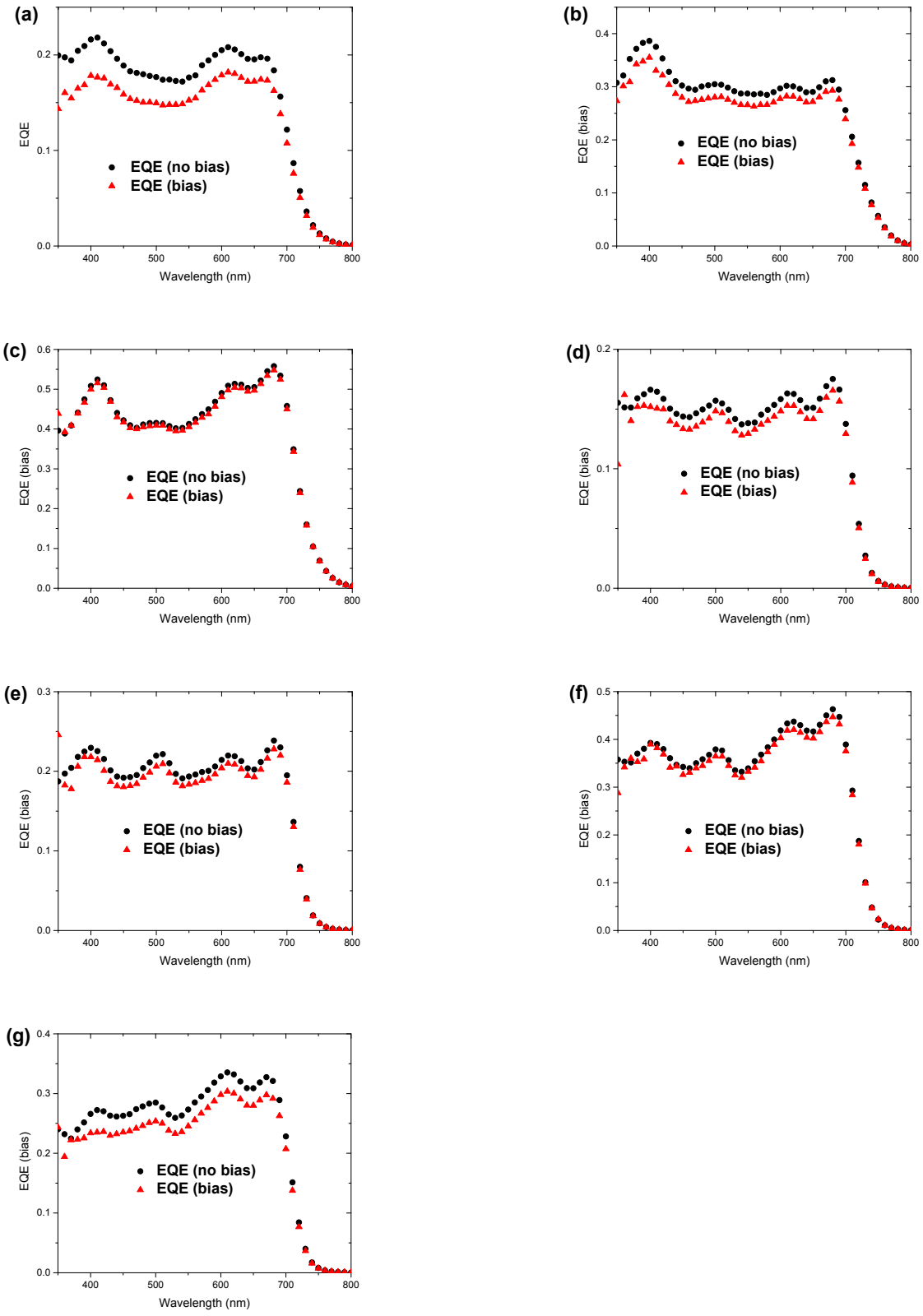

Fig. S6 EQEs measured with and without optical bias of the polymer:[60]PCBM solar cells based on BDT-BT-C40 (a), BDT-BT-C32 (b), BDT-BT-C24 (c), BDT-FBT-C40 (d), BDT-FBT-C32 (e), BDT-FBT-C24 (f), and BDT-FBT-C20 (g).

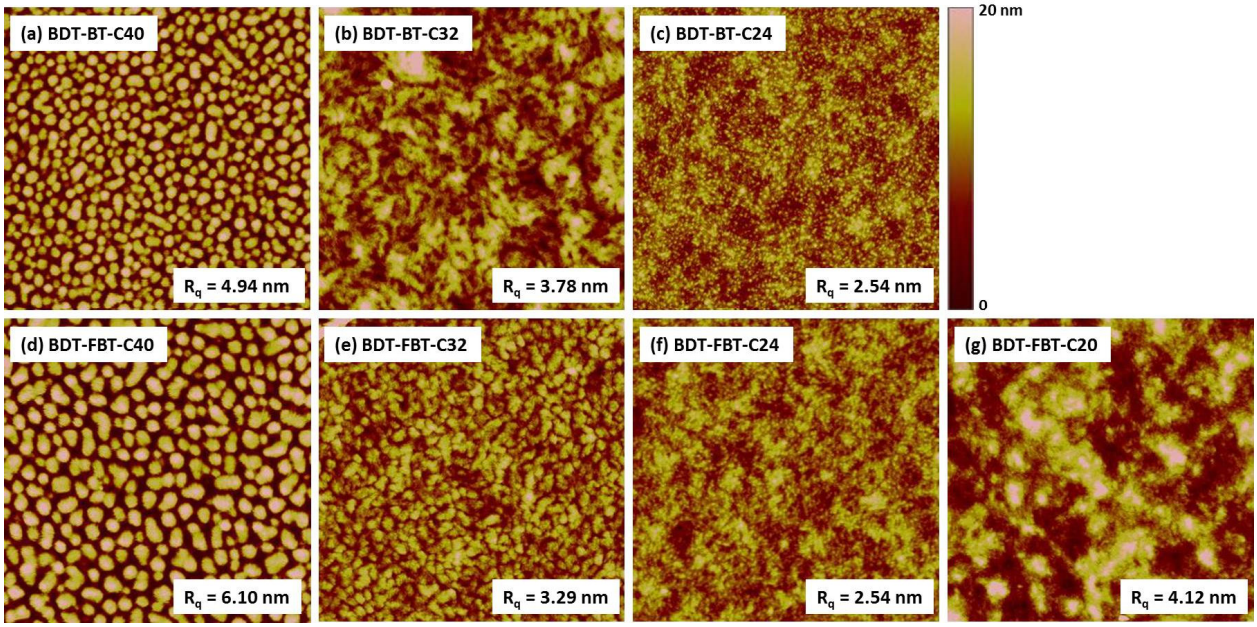

Fig. S7 AFM height images (5×5 μm^2, vertical scale 20 nm) of the polymer:[60]PCBM blend films spin-coated from CB for BDT-BT-C40 (a), BDT-BT-C32 (b), BDT-BT-C24 (c), BDT-FBT-C40 (d), BDT-FBT-C32 (e), BDT-FBT-C24 (f), and BDT-FBT-C20 (g). The root mean square roughness (R_q) of these films is 4.94, 3.78, 2.54, 6.10, 3.29, 2.54, and 4.12 nm from (a) to (g).

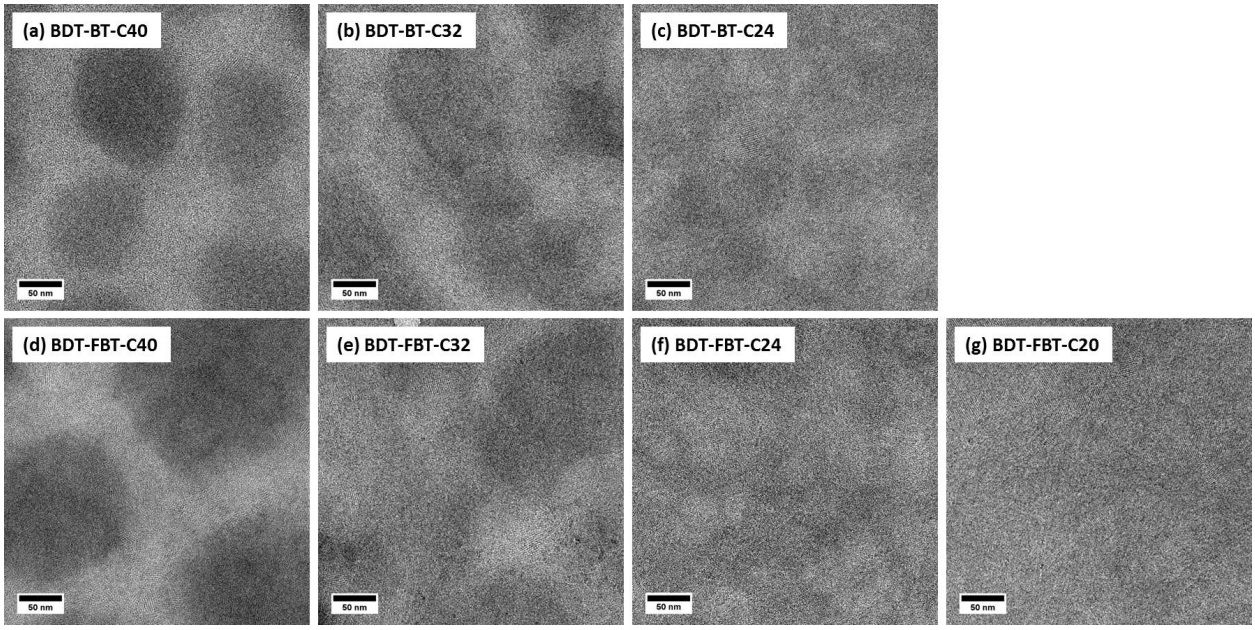

Fig. S8 Bright field TEM images of the polymer:[60]PCBM blend films spin-coated from CB for BDT-BT-C40 (a), BDT-BT-C32 (b), BDT-BT-C24 (c), BDT-FBT-C40 (d), BDT-FBT-C32 (e), BDT-FBT-C24 (f), and BDT-FBT-C20 (g). Image size: 350×350 nm^2; scale bar: 50 nm.

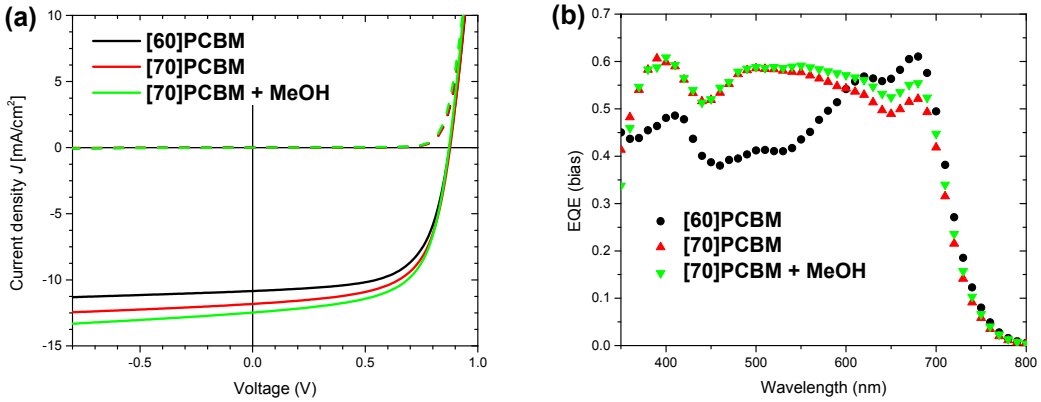

Fig. S9 Current density − voltage characteristics of the solar cells based on BDT-BT-C24 processed from CB (2.5% DIO) under AM1.5G illumination (100 mW cm^{-2}); (b) EQE curves of the corresponding solar cells.

Table S3 Performance parameters of the solar cells based on BDT-BT-C24 processed from CB (2.5% DIO) under AM1.5G illumination (100 mW cm^{-2}). The device structure is ITO/PEDOT:PSS/BDT-BT-C24:fullerene/PFN/Al.

Fullerene	J_{sc} (mA cm^{-2})	V_{oc} (V)	FF (-)	PCE (%)	EQE_{max} (-)
[60]PCBM	10.9	0.87	0.64	6.1	0.61
[70]PCBM	11.8	0.88	0.63	6.5	0.61
[70]PCBM + MeOH	12.3	0.87	0.63	6.8	0.61